Journal of Solid State Chemistry **158,** 169–174 (2001)
doi:10.1006/jssc.2001.9088, available online at http://www.idealibrary.com on IDEAL®

Structural and Electrochemical Study of $Li_{0.5}Mn_{0.5}Ti_{1.5}Cr_{0.5}(PO_4)_3$

A. Aatiq,*,† C. Delmas,*,[1] and A. El Jazouli†

*Institut de Chimie de la Matière Condensée de Bordeaux, CNRS and Ecole Nationale Supérieure de Chimie et Physique de Bordeaux, Château de Brivazac, Av. du Dr A. Schweitzer, 33608 Pessac Cedex, France; and †Laboratoire de Chimie des Matériaux Solides, Faculté des Sciences Ben M'Sik, Avenue Idriss El harti, 7955 Casablanca, Morocco

Received July 26, 2000; in revised form January 3, 2001; accepted January 19, 2001

Materials from the $Li_{(1-x)}Mn_xTi_{(2-x)}Cr_x(PO_4)_3$ ($x = 0$, 0.5, 1) solid solution were obtained by solid state reaction. The structure of the selected $Li_{0.5}Mn_{0.5}Ti_{1.5}Cr_{0.5}(PO_4)_3$ composition was determined from X-ray diffraction data using Rietveld analysis. It is similar to that of $MnTiCr(PO_4)_3$ (space group $R\bar{3}c$) with the Ti and Cr atoms in the Nasicon framework, while the Mn atoms are statistically distributed in the M1 sites. A comparative study of lithium intercalation in $LiTi_2(PO_4)_3$, $Mn_{0.5}Ti_2(PO_4)_3$, and $Li_{0.5}Mn_{0.5}Ti_{1.5}Cr_{0.5}(PO_4)_3$ clearly illustrates that only the M2 sites are involved in the intercalation for $Li_{0.5}Mn_{0.5}Ti_{1.5}Cr_{0.5}(PO_4)_3$, showing thus that in the pristine material the M1 sites are fully occupied by 0.5 Li atom and 0.5 Mn atom.

1. INTRODUCTION

Nasicon-type materials with the general formula $A_nB_2(PO_4)_3$ have received considerable attention because of their interesting physical properties (1–7). The structure consists of a 3D network built up of corner-sharing PO_4 tetrahedra and BO_6 octahedra with large interconnected channels where the A cations are inserted in two types of sites, usually labelled M1 and M2. Since most of the studies concern the ionic conductivity properties, materials with alkali ions localized in these sites have often been considered. However, it must be pointed out that divalent cations can also occupy these sites (8, 9). Recently we have undertaken a general study of the Mn-Nasicon-type materials; the structure determination of $Mn_{0.5}Ti_2(PO_4)_3$, $LiMn_{0.5}TiCr(PO_4)_3$, and $MnTiCr(PO_4)_3$ was reported (10, 11). In all these materials, the Mn^{2+} ions are located in the M1 sites. The structure of $MnTiCr(PO_4)_3$ is isotypic of the $LiTi_2(PO_4)_3$ one (space group $R\bar{3}c$) (11–13). Our structural study on the $Li_{(1-x)}Mn_xTi_{(2-x)}Cr_x(PO_4)_3$ ($0 \le x \le 1$) solid solution is reported in the present paper.

[1] To whom correspondence should be addressed. Fax: + 33-5-5584-6634. E-mail: delmas@icmcb.u-bordeaux.fr.

The presence of interstitial sites offers the possibility of cation intercalation into the Nasicon-type structure. Many references can be found in the literature on chemical and electrochemical lithium intercalation in $A_nB_2(XO_4)_3$ phases, either when the A sites are occupied by monovalent cations such as Li^+ or Na^+ or when they are empty as in the case of $NbTi(PO_4)_3$ or $FeTi(SO_4)_3$ (7, 14–24); in contrast, little information is available about electrochemical lithium intercalation in these Nasicon-type materials when the M1 sites are partially or fully occupied by bulky immobile ions such as Mn^{2+}.

Some of the previous works have shown that the Nasicon-type materials look promising as positive electrode materials for lithium batteries. This material family can be used for the mapping of transition metal redox potentials in relation to the nature of the counter atom X (in XO_4). In fact, the position of the redox potentials with respect to the Fermi energy of lithium was determined electrochemically for several transition metals during lithium intercalation. For instance, in Nasicon phosphate materials, the following positions were found for the redox couples: V^{4+}/V^{3+} at 3.8 eV, Fe^{3+}/Fe^{2+} at 2.8 eV, Ti^{4+}/Ti^{3+} at 2.5 eV, Nb^{5+}/Nb^{4+} at 2.2 eV, Nb^{4+}/Nb^{3+} at 1.8 eV, and V^{3+}/V^{2+} at 1.7 eV (7, 16–22). Moreover, in previous work, we showed that lithium intercalation in $LiTi_2(PO_4)_3$, $Mn_{0.5}Ti_2(PO_4)_3$, and $LiMn_{0.5}TiCr(PO_4)_3$ Nasicon-type phases can give interesting insight about the sites available within the framework (7, 11, 13). In order to obtain more precise structural information for the $Li_{0.5}Mn_{0.5}Ti_{1.5}Cr_{0.5}(PO_4)_3$ material, we have used the Rietveld refinement of X-ray diffraction patterns and the study of electrochemical lithium intercalation as complementary methods.

2. EXPERIMENTAL

Syntheses of $Li_{(1-x)}Mn_xTi_{(2-x)}Cr_x(PO_4)_3$ ($x = 0$, 0.5, 1) were carried out using conventional solid-state reaction techniques. Powder crystalline samples were prepared from mixtures of ($MnCO_3xH_2O$), TiO_2, Cr_2O_3, $NH_4H_2PO_4$, and Li_2CO_3, in stoichiometric proportions. The mixtures

0022-4596/01 $35.00

were heated progressively with intermittent grindings at 200°C (24 h), 600°C (24 h), 900°C (48 h), and 1000°C (48 h) in air. The X-ray diffraction data were collected at room temperature with a Philips PW 1820 diffractometer (Cu$K\alpha$) equipped with a diffracted beam monochromator. The data were collected in the 14–120° range in steps of 0.02° (2θ), with a constant counting time of 40 s per step. The refinement of the structure by the Rietveld method was performed using the Fullprof program (25).

Electrochemical intercalation was carried out in lithium cells with the following electrochemical chain: Li/$LiClO_4$ (1 M) (in propylene carbonate)/Nasicon (70 wt%) + graphite (28 wt%) + polytetrafluoroethylene (2 wt%). Cells were assembled in an argon-filled dry box and galvanostatically cycled under low current density ($j = 40\ \mu A/cm^2$ for an active mass of 15 mg) at room temperature, with a homemade cycling system managed by an HP 1000 computer (26). For the OCV experiments, in order to be as close as possible to the equilibrium conditions, the relaxation was interrupted when the slope of the $V = f(t)$ curve was equal to 1 mV/h. For the structural characterization of electrochemically intercalated materials, larger cells were built without polytetrafluoroethylene ($j = 20\ \mu A/cm^2$ for an active mass of 80 mg).

3. RESULTS AND DISCUSSION

3.1. X-Ray Diffraction Study

The X-ray diffraction analysis of $Li_{(1-x)}Mn_x Ti_{(2-x)}Cr_x(PO_4)_3$ ($x = 0$, 0.5) shows that these materials are isostructural with $MnTiCr(PO_4)_3$, which crystallizes in the rhombohedral system, space group: $R\bar{3}c$ (11). The progressive substitution of manganese for lithium and of chromium for titanium leads to an increase of the $c_{hex.}$ hexagonal parameter and to a slight decrease of the $a_{hex.}$ parameter (Table 1). In order to determine the effect of manganese and chromium substitution in $LiTi_2(PO_4)_3$, we focused our attention on the $Li_{0.5}Mn_{0.5}Ti_{1.5}Cr_{0.5}(PO_4)_3$ composition, which appears to be representative of the general behavior of the $Li_{(1-x)}Mn_xTi_{(2-x)}Cr_x(PO_4)_3$ ($0 < x < 1$) system. The manganese, chromium, and titanium cationic distribution was studied by Rietveld analysis.

As we have already deduced from the structural refinement of $MnTiCr(PO_4)_3$, the Ti^{4+} and Cr^{3+} ions in

TABLE 1

	a (Å) (± 0.001)	c (Å) (± 0.002)	V (Å^3) (± 1)
$LiTi_2(PO_4)_3$	8.510	20.857	1308
$Li_{0.5}Mn_{0.5}Ti_{1.5}Cr_{0.5}(PO_4)_3$	8.500	20.926	1309
$MnTiCr(PO_4)_3$	8.489	20.955	1308

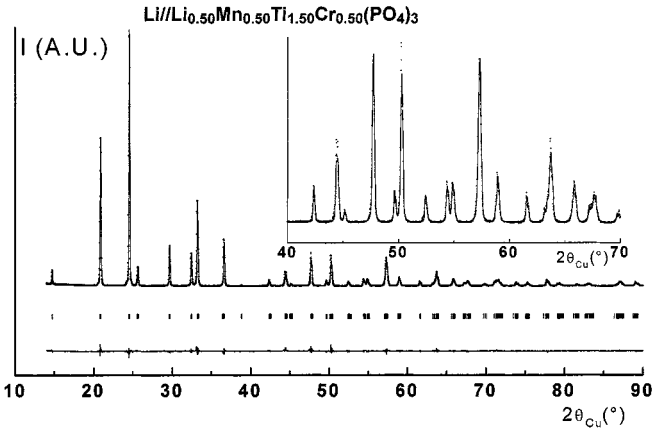

FIG. 1. Comparison of the observed (···) and calculated (—) XRD profiles for $Li_{0.5}Mn_{0.5}Ti_{1.5}Cr_{0.5}(PO_4)_3$. The difference pattern is also given.

$Li_{0.5}Mn_{0.5}Ti_{1.5}Cr_{0.5}(PO_4)_3$ are assumed to be statistically distributed within the B octahedral sites of the $B_2(PO_4)_3$ framework. As was found for the Mn-Nasicon compounds $Mn_{0.5}Ti_2(PO_4)_3$, $MnTiCr(PO_4)_3$ and $LiMn_{0.5}TiCr(PO_4)_3$ (10, 11), the Mn atoms are supposed to occupy only the M1 site. Note that for the materials involved in the present study, the $R\bar{3}c$ space group leads to a statistical distribution of Mn^{2+} ions within the M1 site, whereas in the case of $Mn_{0.5}Ti_2(PO_4)_3$ ($R\bar{3}$ space group), the Mn^{2+} ions are ordered in every other M1 site along the c-axis (10). The atomic positions in $MnTiCr(PO_4)_3$ were used as starting parameters for the Rietveld refinement of $Li_{0.5}Mn_{0.5}Ti_{1.5}Cr_{0.5}(PO_4)_3$. The refinement was done in two steps. In the first, the lithium ions were ignored: this structural model leads to satisfactory reliability factors ($R_{WP} = 10.2\%$, $R_B = 4.2\%$). As a consequence of the very small atomic diffusion factor of Li^+ ions, the Rietveld refinement using XRD data does not permit the location of lithium without ambiguity. As will be shown later, an electrochemical study has demonstrated that the Li^+ ions in $Li_{0.5}Mn_{0.5}Ti_{1.5}Cr_{0.5}(PO_4)_3$ are localized in the M1 site. In a second step, the Rietveld analysis was thus performed with the lithium ions in the M1 site. As expected, this second hypothesis leads to a small improvement of the reliability factors ($R_{WP} = 9.9\%$; $R_B = 3.5\%$). the atomic positions of Mn, Ti, Cr, and O remain very similar in the two hypotheses. The fitted X-ray diffraction profile and the results of the Rietveld refinement are given in Fig. 1 and Table 2, respectively. The refinement assuming the presence of lithium ions in the M2 site does not lead to an improvement of the relationability factors. Moreover, this hypothesis is not expected since the corner-sharing Nasicon structure tends to favor the occupation of only one type of sites if the chemical formula allows it.

Figure 2 shows perspective views of part of the Nasicon ribbon in $LiTi_2(PO_4)_3$, $Li_{0.5}Mn_{0.5}Ti_{1.5}Cr_{0.5}(PO_4)_3$, MnTi

TABLE 2

$Li_{0.50}Mn_{0.50}Ti_{1.50}Cr_{0.50}(PO_4)_3$
Space group, $R\bar{3}c$ Constraints: $B(Mn) = B(Li)$
$a_{hex.} = 8.500(1)$ Å $B(Ti) = B(Cr)$
$c_{hex.} = 20.926(2)$ Å

Atom	Site	Wyckoff positions			Occupancy	B(Å^2)
Mn	6*b*	0	0	0	0.50	1.1(1)
Li	6*b*	0	0	0	0.50	1.1(1)
Ti	12*c*	0	0	0.1427(2)	0.75	0.46(3)
Cr	12*c*	0	0	0.1427(2)	0.25	0.46(3)
P	18*e*	0.289(4)	0	0.25	1	0.61(1)
O(1)	36*f*	0.1829(4)	0.9946(8)	0.1885(2)	1	1.27(1)
O(2)	36*f*	0.1835(6)	0.1616(6)	0.0807(2)	1	0.64(1)

Conditions of the Run

Temperature	300 K
Angular range	$14^\circ \le 2\theta \le 120^\circ$
Step scan increment (2θ)	0.02°
Zero point (2θ)	$-0.0043(4)^\circ$
Number of fitted parameters	28

Profile Parameters

Pseudo-Voigt function	
$PV = \eta L + (1\text{-}\eta)G$	$\eta = 0.544(7)$
Half-width parameters	$U = 0.092(5)$
	$V = -0.002(1)$
	$W = 0.004(1)$

Conventional Rietveld R-Factors for Points with Bragg Contribution
$R_{wp} = 9.9\%$; $R_B = 3.5\%$

Note. Standard deviations have been multiplied by the Scor number (2.4) to correct from local correlations (25).

$Cr(PO_4)_3$, and $Mn_{0.5}Ti_2(PO_4)_3$. In $Li_{0.5}Mn_{0.5}Ti_{1.5}Cr_{0.5}(PO_4)_3$, the Li(Mn)–O2 distance between the cation at the center of the M1 site (6*b* position) and the surrounding O2 oxygen atoms (36*f* position) is equal to 2.24 Å, which is intermediate between the Mn–O2 distance in $MnTiCr(PO_4)_3$ (2.22 Å) and the Li–O2 one in $LiTi_2(PO_4)_3$ (2.26 Å) (Table 3). Therefore, the Li(Mn)–O2 distance in $Li_{0.5}Mn_{0.5}Ti_{1.5}Cr_{0.5}(PO_4)_3$ appears to be in good agreement with the statistical occupancy of the M1 site by Mn and Li atoms. Note that the $c_{hex.}$ parameter increases when Li^+ ions in $LiTi_2(PO_4)_3$ are replaced by Mn^{2+} ions, as expected from the difference in ionic radii ($R^+_{Li} = 0.74$ Å and $R^{2+}_{Mn} = 0.83$ Å for an octahedral environment (27)). In $Li_{0.5}Mn_{0.5}Ti_{1.5}Cr_{0.5}(PO_4)_3$ and $MnTiCr(PO_4)_3$, the distortions of the $Ti(Cr)O_6$ octahedra are similar; they are greater than the TiO_6 ones in the case of $LiTi_2(PO_4)_3$. This is due to the stronger electrostatic repulsion between Ti(Cr) and the divalent manganese ions in comparison to the Ti–Li one. In the case of $Mn_{0.5}Ti_2(PO_4)_3$, the ordered distribution of manganese and vacancies along the ribbon leads to a large distortion for half the TiO_6 octahedra which are in the vicinity of the Mn^{2+} ions and to almost no distortion for the TiO_6 octahedra which are close to the vacancies (Table 3). The comparison of all these structural data suggests that the lithium ions are in the M1 site in $Li_{0.5}Mn_{0.5}Ti_{1.5}Cr_{0.5}(PO_4)_3$. In fact, if vacancies were present in the M1 site, the TiO_6 distortion would be expected to be intermediate between those observed for $Mn_{0.5}Ti_2(PO_4)_3$ (10, 13).

Rietveld refinement using XRD data does not permit distinction between Ti, Cr, and Mn atoms. Nevertheless, the Li(Mn)–O and Ti(Cr)–O distances, which are in good agreement with the ionic radii values ($R^{4+}_{Ti} = 0.605$ Å, $R^{3+}_{Cr} = 0.615$ Å, $R^{2+}_{Mn} = 0.83$ Å, $R^+_{Li} = 0.76$ Å, $R^{2-}_{O} = 1.40$ Å) (27), clearly show that the Ti and Cr atoms are distributed within the framework whereas the Mn atoms occupy the M1 site. The PO_4 tetrahedra are regular with a P–O average distance of 1.56(1) Å, this value fitting well with those typically observed in Nasicon-type phosphates.

3.2. *Electrochemical Intercalation Study*

The electrochemical intercalation study was carried out using $Li//Li_{(0.5+y)}Mn_{0.5}Ti_{1.5}Cr_{0.5}(PO_4)_3$ cells. The OCV curve obtained for the first discharge is reported in Fig. 3 in comparison to those of $LiTi_2(PO_4)_3$ and $Mn_{0.5}Ti_2(PO_4)_3$. In previous studies, we have shown that the filling of the M2 site in titanium-based Nasicon phases leads to a potential close to 2.5 V (7, 13, 28). This value was especially well shown in the case of the $LiTi_2(PO_4)_3$–$Li_3Ti_2(PO_4)_3$ system, for which a neutron diffraction study showed that the M1 site is completely occupied for $LiTi_2(PO_4)_3$ and completely empty for $Li_3Ti_2(PO_4)_3$ (28). Very recent reinvestigation of this system showed that in the latter material, the lithium ions are not in the center of the M2 site, but occupy a distorted tetrahedral site (M3) localized between M2 and M1 (28) as was recently found for $Li_3Fe_2(PO_4)_3$ and $Li_3V_2(PO_4)_3$ (22, 29).

In the case of $Mn_{0.5}Ti_2(PO_4)_3$, the filling of half the M1 sites that were initially empty ($[Mn_{0.5}\square_{0.5}]_{M1}Ti_2(PO_4)_3$) leads to a potential plateau in the vicinity of 2.8–3.0 V. Note that when the $[Li_{0.5}Mn_{0.5}]_{M1}Ti_2(PO_4)_3$ composition is exceeded, lithium ions are intercalated further into the M2 site and a 2.5–2.2 V voltage range is obtained. This difference in cell voltage related to lithium intercalation in M1 and M2 sites was also found in the $Li_yMn_{(0.5+x)}Ti_{(2-2x)}Cr_{2x}(PO_4)_3$ ($0 \le x \le 0.50$) system, where the number of lithium ions which can be intercalated in the vicinity of 3 V is equal to the number of vacancies ($0.5 - x$) in the M1 site (13). A general comparison of all these experiments and the similarity between the observed potentials suggest that the lithium ions intercalated in $Li_{0.5}Mn_{0.5}Ti_{1.5}Cr_{0.5}(PO_4)_3$ occupy the M2 site. Therefore, one can assume that in this phase, the M1 sites are fully occupied.

These electrochemical data indicate also that $Li_{0.5}Mn_{0.5}Ti_{1.5}Cr_{0.5}(PO_4)_3$ can intercalate 1.5 mole of Li^+ ions per

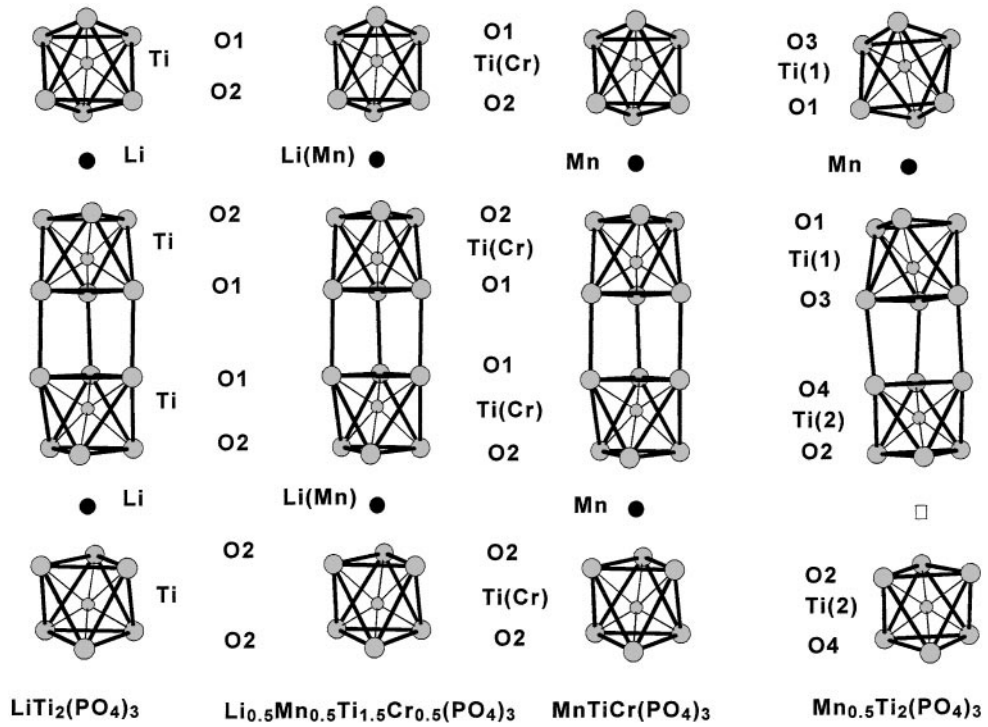

FIG. 2. Cationic distributions observed in the ribbons of $LiTi_2(PO_4)_3$, $Li_{0.5}Mn_{0.5}Ti_{1.5}Cr_{0.5}(PO_4)_3$, $MnTiCr(PO_4)_3$, and $Mn_{0.5}Ti_2(PO_4)_3$.

formula unit, to give $Li_2Mn_{0.5}Ti_{1.5}Cr_{0.5}(PO_4)_3$ in OCV experiments. This intercalation corresponds to the reduction of all the titanium ions to the trivalent state. The powder XRD patterns of the $Li_{(0.5+y)}Mn_{0.5}Ti_{1.5}Cr_{0.5}(PO_4)_3$ ($y = 0$. 1.5) phases are compared in Fig. 4. After intercalation, the crystallinity remains good although a slight broadening of the diffraction lines appears. The hexagonal cell parameters of $Li_2Mn_{0.5}Ti_{1.5}Cr_{0.5}(PO_4)_3$ ($a_{hex.} = 8.510(1)$ Å; $c_{hex.} = 20.949(2)$ Å) show a very slight variation in comparison to those of the $Li_{0.5}Mn_{0.5}Ti_{1.5}Cr_{0.5}(PO_4)_3$ starting phase. At this point, one question arises: does the 0.5 lithium ion present in the starting material remain in the M1 site or does it move to the M2 site? These two hypotheses lead to the following cationic distributions: $[Li_{0.5}Mn_{0.5}]_{M1}[Li_{1.5}]_{M2}Ti_{1.5}Cr_{0.5}(PO_4)_3$ and $[\square_{0.5}Mn_{0.5}]_{M1}[Li_2]_{M2}Ti_{1.5}Cr_{0.5}(PO_4)_3$. (In this study, due to the lack of neutron diffraction experiment, the Li^+ ions are considered to occupy the center of the M2 site even if some subsites can in fact be occupied.) The electrochemical behavior cannot discriminate between these two hypotheses. But, the comparison of the variation of the $c_{hex.}$ parameter upon lithium intercalation with that observed for the $Li_yMn_{0.5}Ti_2(PO_4)_3$ system suggests that the M1 site is fully occupied in the $Li_2Mn_{0.5}Ti_{1.5}Cr_{0.5}(PO_4)_3$ phase. As a matter of fact, the variation in the $c_{hex.}$ parameter results from the presence or lack of vacancies in the M1 site and from the thickness of the

TABLE 3

	A–O2	A–Ti, A–Ti(Cr)	Ti–Ti, Ti(Cr)–Ti(Cr)	Ti–O1, Ti(Cr)–O1	Ti–O2, Ti(Cr)–O2
$LiTi_2(PO_4)_3$	2.261(5)	2.948(7)	4.535(7)	1.867(7)	1.937(7)
$Li_{0.5}Mn_{0.5}Ti_{1.5}Cr_{0.5}(PO_4)_3$	2.243(8)	2.985(7)	4.490(7)	1.847(7)	1.964(7)
$MnTiCr(PO_4)_3$	2.225(8)	3.006(7)	4.468(7)	1.867(7)	1.989(7)
$[\square_{0.5}Mn_{0.5}]Ti_2(PO_4)_3$		Ti(2)–O2	1.859(4)[a]		
		Ti(2)–O4	1.863(6)[b]		
		Ti(1)–O1	2.022(4)[b]		
		Ti(1)–O3	1.865(6)[b]		

[a]Around vacant (□) M1 site.
[b]Around occupied (Mn) M1 site.

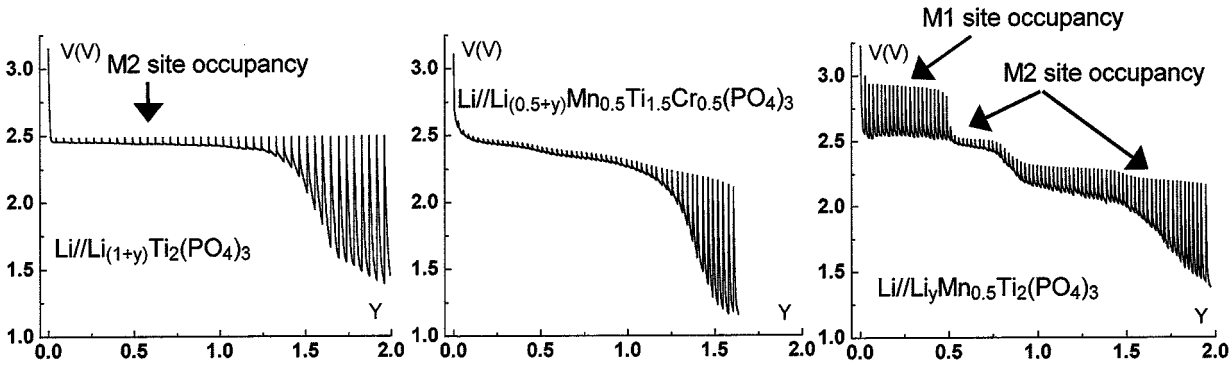

FIG. 3. OCV discharge curves $V(V) = f(y)$ for $Li/Li_{(1+y)}Ti_2(PO_4)_3$, $Li//Li_{(0.5+y)}Mn_{0.5}Ti_{1.5}Cr_{0.5}(PO_4)_3$, and $Li//Li_yMn_{0.5}Ti_2(PO_4)_3$ cells ($j = 40\ \mu A/cm^2$; end of relaxation, 1 mV/h).

$Ti(Cr)O_6$–$Ti(Cr)O_6$ units, which is directly related to the oxidation state of the 3*d* element (Fig. 2). In the case of the $Li_yMn_{0.5}Ti_2(PO_4)_3$ system, a 0.14 Å decrease of the $c_{hex.}$ parameter is observed when Li^+ ions occupy the vacancies of the starting material for $y = 0.5$, although there is a partial reduction of titanium ions which leads to larger TiO_6 octahedra (Table 4). If vacancies were present in half the M1 sites of the $Li_2Mn_{0.5}Ti_{1.5}Cr_{0.5}(PO_4)_3$ phase, the increase of the $c_{hex.}$ parameter would be considerably larger than the one observed because the two contributions would act in the same way.

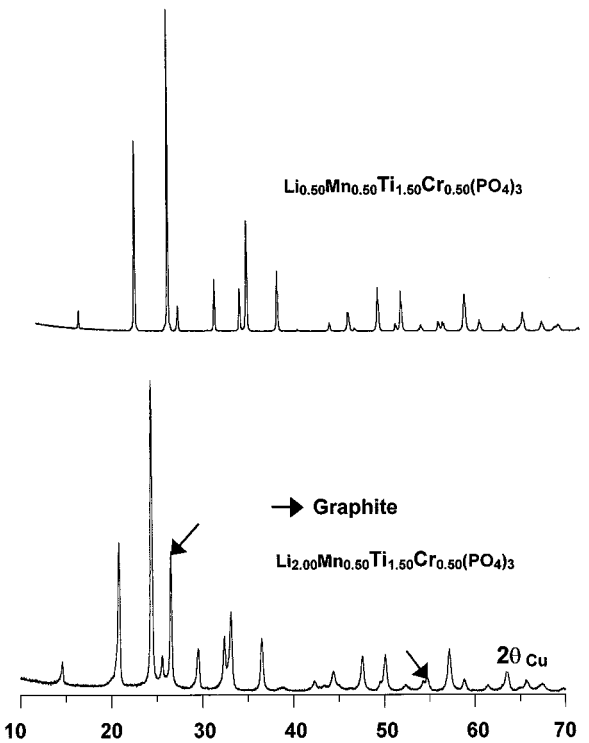

FIG. 4. XRD patterns of the $Li_{(0.5+y)}Mn_{0.5}Ti_{1.5}Cr_{0.5}(PO_4)_3$ ($y = 0.0$, 1.5) phases.

Cycling experiments were performed for $Li//Li_{(0.5+y)}Mn_{0.5}Ti_{1.5}Cr_{0.5}(PO_4)_3$ batteries under two current densities (40 and 100 $\mu A/cm^2$) between 2.1 and 3.5 V (Fig. 5). Electrochemically, 1.1 lithium atom per formula unit could be inserted into the structure at 40 $\mu A/cm^2$ corresponding to a capacity of 70 mAh/g. An increase of the current density to 100 $\mu A/cm^2$ results in a decrease of the capacity from 70 mAh/g to 50 mAh/g. In both cases, a good reversibility is observed; almost all the intercalated lithium ions can be deintercalated in the vicinity of 2.5 V. There is almost no capacity between 2.7 and 3.5 V. These two facts show that during the charge process there is no lithium deintercalation from the M1 site even if this site is necessarily involved in the long-range diffusion process required by the intercalation (deintercalation) reaction. After 40 cycles, the reversibility of the intercalation–deintercalation phenomenon as well as the structural integrity was maintained.

4. CONCLUSION

Rietveld refinement of the XRD pattern and lithium intercalation were used as complementary methods to characterize the distribution of lithium and manganese ions in $Li_{0.5}Mn_{0.5}Ti_{1.5}Cr_{0.5}(PO_4)_3$. It was shown that Li and Mn occupy statistically the M1 sites and that the lithium ions electrochemically intercalated in this structure are localized in the M2 site. Neutron diffraction experiments are in progress to unambiguously confirm these results.

TABLE 4

	$a_{hex.}$ (Å) ($\pm$ 0.001)	$c_{hex.}$ (Å) ($\pm$ 0.002)
$[\square_{0.5}Mn_{0.5}]_{M1}Ti_2(PO_4)_3$	8.510	21.087
$[Li_{0.5}Mn_{0.5}]_{M1}Ti_2(PO_4)_3$	8.535	20.949
$Li_{0.5}Mn_{0.5}Ti_{1.5}Cr_{0.5}(PO_4)_3$	8.500	20.926
$Li_2Mn_{0.5}Ti_{1.5}Cr_{0.5}(PO_4)_3$	8.510	20.949

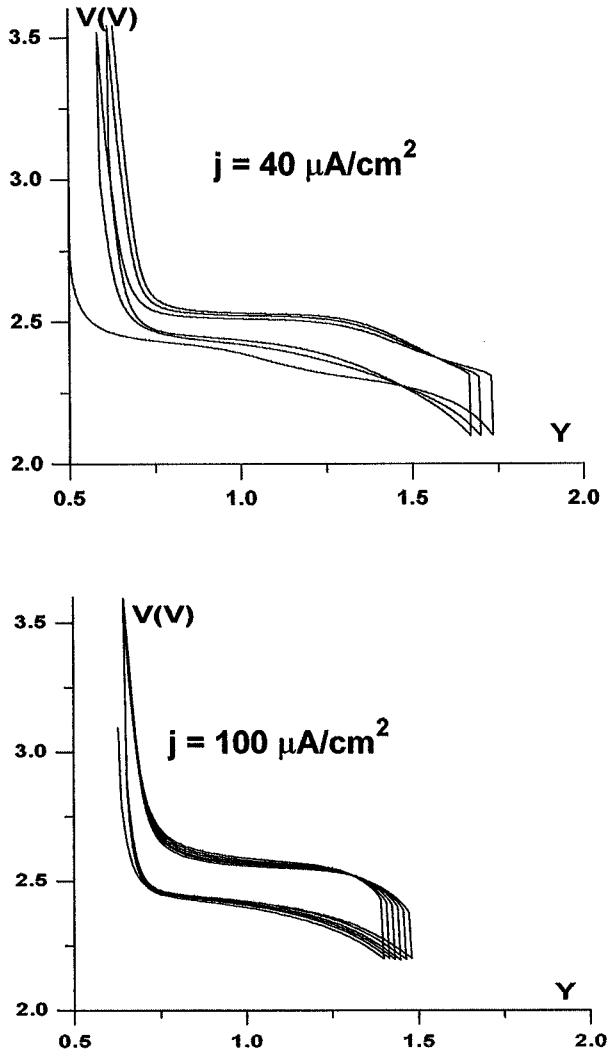

FIG. 5. Cycling of a Li//$Li_{(0.5+y)}Mn_{0.5}Ti_{1.5}Cr_{0.5}(PO_4)_3$ cell under two current densities ($j = 40\ \mu A/cm^2$, C/24 rate; $j = 100\ \mu A/cm^2$, C/7 rate).

ACKNOWLEDGMENTS

The authors thank M. Ménétrier and L. Croguennec for fruitful discussions, C. Denage for technical assistance, and Région Aquitaine for financial support.

REFERENCES

1. H. Y.-P. Hong, *Mater. Res. Bull.* **11,** 173, (1976).
2. J. B. Goodenough, H. Y.-P. Hong, and J. A. Kafalas, *Mater. Res. Bull.* **11,** 203 (1976).
3. F. Cherkaoui, J. C. Viala, C. Delmas, and P. Hagenmuller, *Solid State Ionics* **21,** 333 (1986).
4. F. D'Yvoire, M. Pintard-Screpel, E. Bretey, and M. G. de la Rochere, *Solid State Ionics* **9–10,** 851 (1983).
5. R. Roy, D. K. Agrawal, J. Alamo, and R. A. Roy, *Mater. Res. Bull.* **19,** 471 (1984).
6. T. Maruyama, S. Sasaki, and Y. Saito, *Solid State Ionics* **23,** 107 (1987).
7. C. Delmas, A. Nadiri, and J. L. Soubeyroux, *Solid State Ionics* **28–30,** 419 (1988).
8. R. Perret and A. Boudjada, *Bull. Soc. Fr. Mineral. Cristallogr.* **100,** 5 (1977).
9. O. Mentre, F. Abraham, B. Deffontaines, and P. Vast, *Solid State Ionics* **72,** 293 (1994).
10. H. Fakrane, A. Aatiq, M. Lamire, A. El Jazouli, and C. Delmas, *Ann. Chim. Sci. Mater.* **23,** 81 (1998).
11. A. Aatiq, C. Delmas, A. El Jazouli, and P. Gravereau, *Ann. Chim. Sci. Mater.* **23,** 121 (1998).
12. R. Masse, *Bull. Soc. Fr. Miner. Cristallogr.* **93,** 500 (1970).
13. A. Aatiq, Thesis, Faculty of Science Ben M'Sik, Casablanca, 1997.
14. O. Tillement, J. C. Couturier, J. Angenault, and M. Quarton, *Solid State Ionics* **48,** 249 (1991).
15. O. Tillement, J. Angenault, J. C. Couturier, and M. Quarton, *Solid State Ionics* **53–56,** 391 (1992).
16. K. S. Nanjundaswamy, A. K. Padhi, J. B. Goodenough, S. Okada, H. Ohtsuka, H. Arai, and J. Yamaki, *Solid State Ionics* **92,** 1 (1996).
17. A. K. Padhi, K. S. Nanjundaswamy, C. Masquelier, and J. B. Goodenough, *J. Electrochem. Soc.* **144**(8), 2581 (1997).
18. A. K. Padhi, K. S. Nanjundaswamy, C. Masquelier, S. Okada, and J. B. Goodenough, *J. Electrochem. Soc.* **144**(5), 1609 (1997).
19. C. Masquelier, A. K. Padhi, K. S. Nanjundaswamy, and J. B. Goodenough, *J. Solid State Chem.* **135,** 228 (1998).
20. A. K. Padhi, V. Manivannan, and J. B. Goodenough, *J. Electrochem. Soc.* **145**(5), 1518 (1998).
21. J. B. Goodenough and V. Manivannan, *Denki. Kagaku* **66**(12), 1173 (1998).
22. K. Yoshida, K. Toda, K. Uematsu, and M. Sato, *Key Eng. Mater.* **157–158,** 289 (1999).
23. L. Znaidi, S. Launay, and M. Quarton, *Solid State Ionics* **93,** 273 (1997).
24. G. B. M. Vaughan, J. Gaubicher, T. Le Mercier, J. Angenault, M. Quarton, and Y. Chabre, *J. Mater. Chem.* **9,** 2809 (1999).
25. J. Rodriguez-Carvajal, Collected Abstracts Powder Diffraction Meeting, Toulouse, 1990, p. 127.
26. A. Mendiboure and C. Delmas, *Comput. Chem.* **11**(3), 153 (1987).
27. R. D. Shannon, *Acta Crystallogr. A* **32,** 751 (1976).
28. A. Aatiq, M. Ménétrier, L. Croguennec, E. Suard, and C. Delmas, *Solid State Ionics* (submitted).
29. C. Masquelier, C. Wurn, J. Rodriguez-Carvajal, J. Gaubicher, and L. Nazar, *Chem. Mater.* **12,** 525 (2000).